ELECTRONIC SUPPLEMENTARY INFORMATION

Unlocking the Effect of Zn^{2+} on Crystal Structure, Optical Properties, and Photocatalytic Degradation of Perfluoroalkyl Substances (PFAS) of Bi_2WO_6

Mirabbos Hojamberdiev[1,*], Ana Laura Larralde[2,3], Ronald Vargas[4,5], Lorean Madriz[4,5], Kunio Yubuta[6], Lokesh Koodlur Sannegowda[7], Ilona Sadok[8], Agnieszka Krzyszczak-Turczyn[8,9], Patryk Oleszczuk[9], and Bożena Czech[9,*]

[1]*Institut für Chemie, Technische Universität Berlin, Straße des 17. Juni 135, 10623 Berlin, Germany*

[2]*Consejo Nacional de Investigaciones Científicas y Técnicas (CONICET), Buenos Aires, Argentina*

[3]*Instituto Nacional de Tecnología Industrial, Avenida General Paz 5445, San Martín (B1650WAB), Buenos Aires, Argentina*

[4]*Instituto Tecnológico de Chascomús (INTECH), Consejo Nacional de Investigaciones Científicas y Técnicas (CONICET), Avenida Intendente Marino, Km 8,2, Chascomús (B7130IWA), Provincia de Buenos Aires, Argentina*

[5]*Escuela de Bio y Nanotecnologías, Universidad Nacional de San Martín (UNSAM), Avenida Intendente Marino, Km 8,2, Chascomús (B7130IWA), Provincia de Buenos Aires, Argentina*

[6]*Department of Applied Quantum Physics and Nuclear Engineering, Kyushu University, Fukuoka 819-0395, Japan*

[7]*Department of Studies in Chemistry, Vijayanagara Sri Krishnadevaraya University, Cantonment, Vinayakanagara, Ballari, 583105, India*

[8]*Department of Chemistry, Institute of Biological Sciences, Faculty of Medicine, The John Paul II Catholic University of Lublin, Konstantynów 1J, 20-708 Lublin, Poland*

[9]*Department of Radiochemistry and Environmental Chemistry, Institute of Chemical Sciences, Faculty of Chemistry, Maria Curie-Skłodowska University in Lublin, 3 Maria Curie-Skłodowska Sq., 20-031 Lublin, Poland*

*Corresponding authors: E-mail addresses: bozena.czech@mail.umcs.pl (B. Czech) and hmirabbos@gmail.com (M. Hojamberdiev)

LC-QTOF/MS – instrumentation and analysis conditions

A 1200 Series high-performance liquid chromatograph (Agilent Technologies) fitted with autosampler, quaternary pump with degasser, column thermostat and coupled to a tandem mass spectrometer (Agilent Technologies 6538 UHD Accurate Mass Q-TOF LC/MS) equipped with a dual ESI ion source was used. The analytical column used was the Zorbax Eclipse Plus C18 rapid resolution HT (2.1 × 50 mm, 1.8 µm). A 3-min linear gradient of aqueous solutions (5 mmol·L^{-1}) of ammonium formate (A) and methanol (B) with an increase from 30% to 60% (3 min post-run at 30% B, 0.3 mL·min^{-1} flow rate, and 40°C column temperature) was used in the chromatographic analyses. The analytes were ionized in the negative ion polarity mode. The temperature of an ion source gas (nitrogen) was 280°C, and the flow rate was 9 L·min^{-1}. The capillary potential, fragmentor, and nebulizer pressure were set to 3500 V, 80 V, and 35 psi, respectively. The ions were acquired in a MS scan mode at 50-1000 *m/z* with a scan rate of 1 scan s^{-1} (number of transients: 5975 and collision energy: 0 eV). Internal mass calibration was enabled using three reference mass ions (112.985587, 301.998139, and 1033.988109). The samples were analyzed in triplicate (injection volume: 5 µL). After the sample injection, the needle was washed with methanol. The quantification was performed on unprotonated ions $[M\text{-}H]^-$. For PFH_xA, an ion of *m/z* = 312.9748 and the isotopically labeled internal standard ($[^{13}C_6]$-PFH_xA) ion of *m/z* = 318.9921 were extracted, respectively. Data acquisition and analysis were performed using Agilent Mass Hunter software versions B.06.01 and B.07.00, respectively. For the quantitative analysis of PFH_xA, each sample was fortified with $^{13}C_6$-PFHxA (0.25 mg·L^{-1}), vortexed, and passed through a 0.22 µm polypropylene (PP) syringe filter (Bioanalytic, Gdańsk, Poland) into the PP chromatographic vial and analyzed using LC-QTOF/MS. An example of the extracted ion chromatograms is presented in Figure S1.

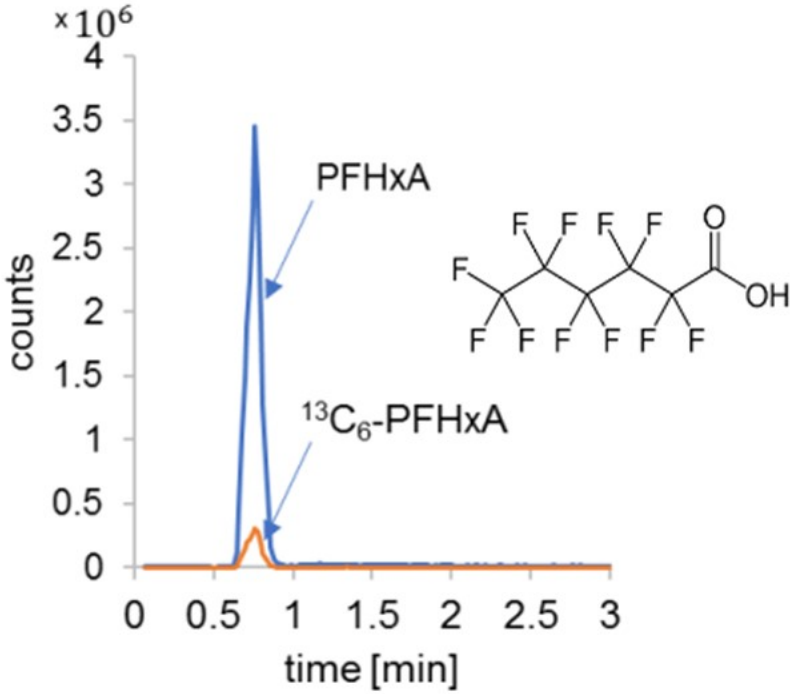

Figure S1. Extracted ion chromatograms of PFH_xA and $^{13}C_6$-PFH_xA.

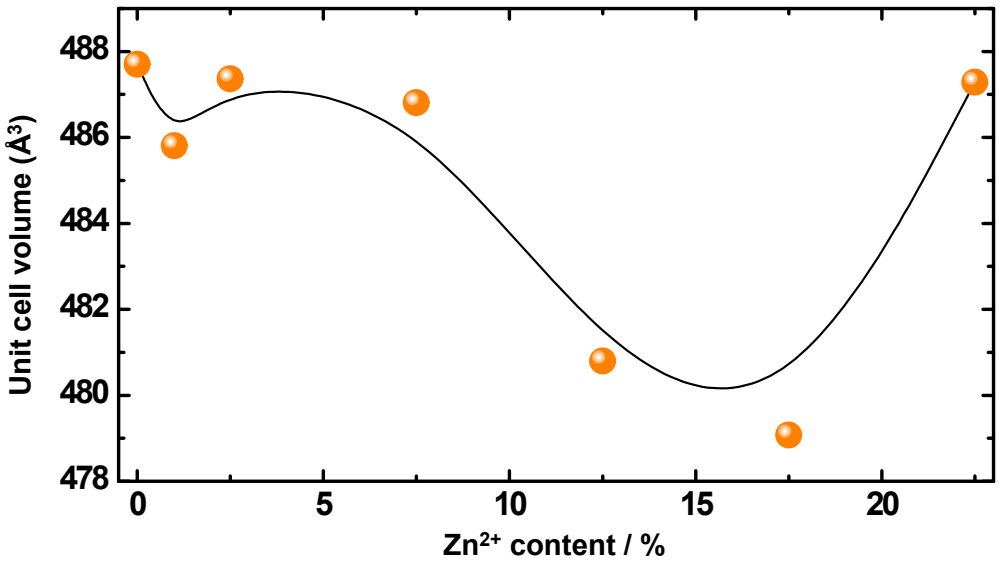

Figure S2. Unit cell volume of $Bi_{2-x}Zn_xWO_{6+\delta}$ as a function of Zn^{2+} content.

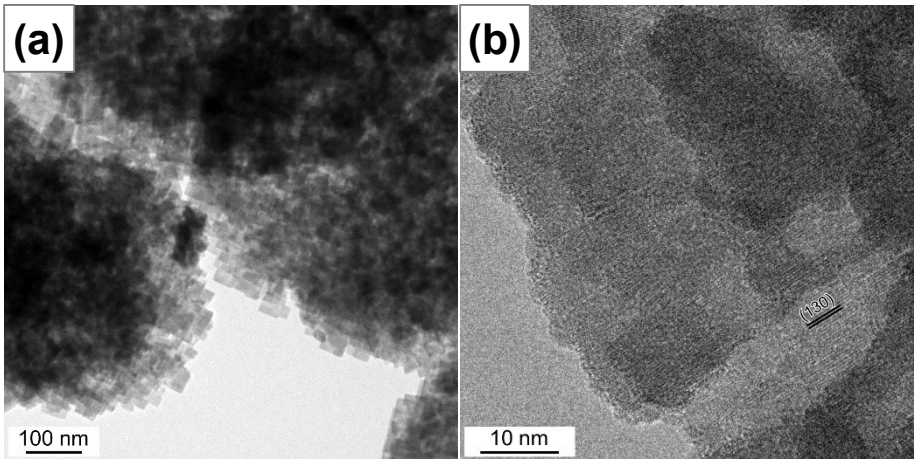

Figure S3. TEM (a) and HRTEM (b) images of Zn17.5.

Table S1. Comparative results of PFAS degradation.

Conditions	Efficiency	Light source	References
Photo-Fenton process	90% degradation and 53.2% defluorination after 5 h	UV	*Chem. Eng. J.*, 2012, **184**, 156–162.
In_2O_3 porous nanospheres	100% within 30 min	UV	*Appl. Catal. B*, 2012, **125**, 350–357.
BiOCl	59.3% defluorination after 3 h	UV	*Chem. Eng. J.*, 2017, **317**, 925–934.
β-Ga_2O_3 nanoplates	100% within 3 h	UV (185 n m)	*Appl. Catal. B*, 2013, **142–143**, 654–661.
In_2O_3	100% decomposition of PFAS	UV	*Chemosphere*, 2017, **189**, 717–729.
Fe/TNTs@AC	>90% decomposition of PFOA in 4 h, of which 62% was completely mineralized to F^-	UV	*Water Res.*, 2020, **185**, 116219.
Iron (Fe^0) nanoparticles	90±1% degradation after 2 h	UV (pH=3.0)	*J. Water Process. Eng.*, 2022, **46**, 102556.
WO_3/TiO_2 catalysts (0–5 wt% WO_3)	4 %–26 % after 4 h	UVA+Vis+ O_3	*Sci. Total Environ.*, 2022, **843**, 157006.
Pb-doped TiO_2 coated with reduced graphene oxide	98% after 24 h	UV	*Water Environ. Res.*, 2023, **95**, e10871.
Hexagonal boron nitride in UVC/VUV system	>99% degradation of PFOA in 15 min and 65% degradation of PFOS in 1 h	UVC (254 nm)	*Environ. Sci. Technol. Lett.*, 2023, **10**, 705–710.
Zn2.5-Bi_2WO_6	57% degradation in 45 min	Visible	This study